AD-A240 496

‖‖‖‖‖‖‖‖‖‖‖‖‖

⟨1⟩

EFFECTS OF HYDROGEN AND CARBON ON THERMALLY ACTIVATED DEFORMATION IN NICKEL

E. Sirois and H.K. Birnbaum
University of Illinois at Urbana-Champaign
Dept. of Materials Science and Engineering
Urbana, IL   61801

DTIC
ELECTE
SEP 19 1991
D
D

Technical Report
August 1991

91-11044

‖‖‖‖‖‖‖‖‖‖‖‖‖

91 9 18   096

REPORT DOCUMENTATION PAGE		READ INSTRUCTIONS BEFORE COMPLETING FORM
1. REPORT NUMBER	2. GOVT ACCESSION NO.	3. RECIPIENT'S CATALOG NUMBER
4. TITLE (and Subtitle) Ffects of Hydrogen and Carbon on Thermally Activated Deformation in Nickel		5. TYPE OF REPORT & PERIOD COVERED
		6. PERFORMING ORG. REPORT NUMBER
7. AUTHOR(s) E. Sirois and H.K. Birnbaum		8. CONTRACT OR GRANT NUMBER(s) N-00014-90-J-1769
9. PERFORMING ORGANIZATION NAME AND ADDRESS University of Illinois Dept. of Materials Science and Engineering Urbana, IL 61801		10. PROGRAM ELEMENT, PROJECT, TASK AREA & WORK UNIT NUMBERS
11. CONTROLLING OFFICE NAME AND ADDRESS Office of Naval Research Arlington, VA		12. REPORT DATE August 1991
		13. NUMBER OF PAGES 35
14. MONITORING AGENCY NAME & ADDRESS(If different from Controlling Office)		15. SECURITY CLASS. (of this report) Unclassified
		15a. DECLASSIFICATION/DOWNGRADING SCHEDULE

16. DISTRIBUTION STATEMENT (of this Report)

This report is unclassified. Reproduction and distribution for any purpose by the U.S. government is permitted.

17. DISTRIBUTION STATEMENT (of the abstract entered in Block 20, if different from Report)

18. SUPPLEMENTARY NOTES

19. KEY WORDS (Continue on reverse side if necessary and identify by block number)

Hydrogen   Plastic deformation
Dislocation
Hydrogen Embrittlement

20. ABSTRACT (Continue on reverse side if necessary and identify by block number)

Deformation experiments were performed to determine the effects of hydrogen and carbon on the activation parameters for dislocation slip in nickel. The techniques used were isothermal stress relaxation and differential temperature measurements. These methods allowed determination of the activation enthalpy and activation area for dislocation motion in nickel and the effects of hydrogen and carbon on these parameters. The results show that hydrogen increases the dislocation mobility in Ni and Ni-C alloys by reducing the activation enthalpy for dislocation motion, while carbon reduces the dislocation

EFFECTS OF HYDROGEN AND CARBON ON THERMALLY ACTIVATED DEFORMATION IN NICKEL

E. Sirois, and H.K. Birnbaum
Department of Materials Science and Engineering
University of Illinois at Urbana-Champaign
Urbana, IL 61801

ABSTRACT

Deformation experiments were performed to determine the effects of hydrogen and carbon on the activation parameters for dislocation slip in nickel. The techniques used were isothermal stress relaxation and differential temperature measurements. These methods allowed determination of the activation enthalpy and activation area for dislocation motion in nickel and the effects of hydrogen and carbon on these parameters. The results show that hydrogen increases the dislocation mobility in Ni and in Ni-C alloys by reducing the activation enthalpy for dislocation motion, while carbon reduces the dislocation mobility by increasing the activation enthalpy. Hydrogen solutes decrease the activation area for dislocation motion in both pure Ni and in Ni-C alloys.

I INTRODUCTION

The effect of hydrogen on the response of metals to stress is generally to decrease the strain to failure and correspondingly to decrease the fracture stress. The mechanism(s) for hydrogen embrittlement are not fully established, but are generally ascribed to a postulated decrease in the atomic bond strength due to hydrogen, i.e. decohesion, or to the effect of hydrogen on the

dislocation behavior, i.e. Hydrogen Enhanced Localized Plasticity (H.E.L.P.). Using environmental cell TEM techniques, direct observations of enhanced dislocation velocities due to H have been made in a number of metals (1-4) and this has been shown to lead to hydrogen related failure by the H.E.L.P. mechanism. Evidence for local plasticity on the fracture surface of hydrogen embrittled macroscopic specimens, e.g. steels (5) and Ni (6), also indicates that hydrogen embrittlement is accompanied by localized plasticity.

There are however, relatively few cases where H in solid solution has been shown to result in a decrease of the flow stress of macroscopic specimens. Softening due to H has been noted in Ni at very low strain rates and low strains (7) when the H was introduced from the gas phase. Electrolytic charging of Ni (8) caused softening and hardening which was associated with formation of a surface hydride or surface damage due to the high stress gradients introduced by cathodic charging. Careful electrolytic charging of H into Fe (9-11) has been shown to result in a significant decrease of the flow stress over a range of temperatures near 300 °K. In contrast to these observations, many cases of increases of the flow stress due to hydrogen have been reported (12-14). In some cases, this flow stress increase can be attributed to near surface damage caused by cathodic charging. In other cases, the increases in yield strength attributed to solute H have been measured at higher strain rates than in the cases where enhanced dislocation motion or decreases in the flow stresses due to H have been observed. Increases in the measured flow stress due

to solute H has been observed simultaneously with slip localization (14) suggesting the possibility of softening along the localized shear bands although macroscopically, the flow stress at the imposed strain rate is increased.

There is little agreement regarding the basic mechanism(s) of these H solute effects on dislocation behavior and plasticity. This paper presents the results of research focused on the effects of hydrogen on thermally activated dislocation motion in macroscopic nickel specimens. Taken together with previous observations, these results allow rationalization of the influence of H on the plastic response of Ni.

I.A Summary of Thermally Activated Dislocation Motion

One of the principle factors which determine the interaction of hydrogen with dislocations is the elastic interaction due to the strain field of the solute atom; measured by a misfit parameter, $\delta = 1/a(\partial a/\partial c)$, where a is the lattice parameter and c is the concentration of the solute. The misfit parameter for carbon in nickel is about 0.21 (15). In Ni, this parameter has been determined to be 0.036 for relatively dilute solutions of hydrogen in nickel (16) and for cathodically charged 310 stainless steel containing 7.1 at.% hydrogen (14) it has been shown to be 0.055. These latter values are, however, considerably smaller than the value of $\delta = 0.079$ derived from a two phase alloy of nickel and nickel hydride obtained by cathodic charging (17). Partial molal volume results tabulated by Peisl (18) for a number of FCC metals and alloys indicate misfit parameters for H in Ni

near 0.05 in reasonable agreement with the results of Refs. (14) and (16). All measurements of this parameter for H in FCC metals, result in values much lower than that for C in Ni. In FCC metals the strain fields of interstitial or substitutional solutes are cubic and therefore the elastic interactions are primarily with the hydrostatic portions of the dislocation stress fields. As a result, the interaction with dislocations, which is proportional to the misfit parameter, will be small for hydrogen and large for carbon.

Experimental observations of solid solution hardening in Ni-C alloys suggest that carbon-dislocation interactions are large and are strongly dependent on temperature (15,19-22). Carbon in solid solution in nickel increases the critical resolved shear stress at a rate of $\delta\sigma/\delta c = \mu/6$ at 4°K and $\mu/32$ at room temperature (21), where c is the carbon concentration and μ is the 4°K shear modulus. Internal friction studies of Ni-C alloys (19) show strong carbon dislocation interactions which were thought to be due to pairs of carbon atoms oriented along <110> directions. These observations have led to the suggestion that the rate controlling mechanism for deformation in Ni-C alloys is dislocation interaction with the asymmetrical strain field of pairs or clusters of carbon atoms (20).

In contrast, the solid solution effects of hydrogen are much smaller with both hardening (7,8,12-14) and softening (7-11) being observed. A hardening rate of $\delta\sigma/\delta c = \mu/4000$ which was recently reported for 310 stainless steel at room temperature (14) exemplifies the weakness of the dislocation-hydrogen interaction in

FCC alloys, where μ is the room temperature shear modulus. Internal friction studies of hydrogen in FCC Ni-Fe alloys (23) and in deformed Ni (24) suggest dislocation interactions with pairs of hydrogen atoms. While the rate controlling mechanism for plastic deformation in Ni-H alloys is not understood, it seems likely that small clusters or atmospheres of hydrogen are involved, as the strain field of a single hydrogen atom is probably insignificant compared to other potential rate controlling obstacles in the lattice.

Another factor which affects the interactions between solutes such as C and H and moving dislocations is the diffusivity of the solutes. The solute atmospheres can drift with moving dislocations at low strain rates or the dislocations can escape the solute atmospheres above a critical dislocation velocity. In this respect C and H differ greatly, with H having a much larger diffusivity at temperatures near 300°K. These dynamic effects of the solute - dislocation interactions are clearly shown in the dynamic strain aging experiments with Ni-H, Ni-C, and Ni-C-H alloys (25).

A technique which can be used to develop an understanding of the individual and combined effects of solid solution carbon and hydrogen in FCC metals is thermal activation analysis (TAA) (26-31). Thermal activation analysis methods can be applied to obtain the activation area, ΔA^*, and the activation enthalpy, ΔH^*, which characterize the thermal activation of a dislocation over short range barriers. This analysis is based upon the description of the rate dependence of deformation described by

$$\dot{\epsilon} = \dot{\epsilon}_0 \exp-((\Delta H^*_0 - \int b\Delta A^* \delta\sigma^*)/kT), \qquad (1)$$

where $\dot{\epsilon}$ is the plastic shear strain rate, $\dot{\epsilon}_0$ is a pre-exponential term given by $\dot{\epsilon}_c = \nu_D \rho_m A \exp(\Delta S^*/k)$, where ν_D is the vibrational attempt frequency, ρ_m is the mobile dislocation density, A is the area swept per activation event, and ΔS^* is the activation entropy. The activation enthalpy, $\Delta H^* = \Delta H^*_0 - \int (b\Delta A^*) \delta\sigma^*$ is the activation enthalpy required to advance a dislocation segment from its stable equilibrium position, A_s, to an unstable equilibrium position, A_u, (from which it can athermally glide forward to the next obstacle) thus sweeping out the area ΔA^*. The total activation enthalpy, ΔH^*_0, is the thermal energy required for activation at zero effective stress, σ^*. The effective stress, σ^*, is defined as the difference between the applied shear stress, σ_A, and the long range internal stress, σ_{LR}, and represents a short range stress acting on the dislocation segment during thermal activation. The absolute temperature is T, k is the Boltzmann constant, and b is the magnitude of the Burgers vector. The activation area term is integrated with respect to the effective stress from zero to σ^*. This formulation allows the activation enthalpy, ΔH^*, to be separated into its stress independent part, ΔH^*_0, and its stress dependent part, $\int b\Delta A^* \delta\sigma^*$.

Experiments designed to measure the activation parameters for thermally activated slip use certain restrictive assumptions and the derivatives of Equation 1. Some of these techniques are listed below:

a) strain rate change at constant temperature:

$$(\delta \ln\dot{\epsilon}/\delta\sigma_A)_{T,S} = b\Delta A^*/kT \qquad (2)$$

b) change in strain rate with temperature at constant stress:

$$(\delta \ln\dot{\epsilon}/\delta T)_{\sigma,S} = \Delta H^*/kT^2 \qquad (3)$$

c) dependence of stress on strain rate combined with the temperature dependence of the flow stress:

$$(\delta \ln\epsilon/\delta\sigma_A)_{T,S}(\delta\sigma_A/\delta T)_{\dot{\epsilon},S} = -\Delta H^*/kT^2 \qquad (4)$$

d) stress relaxation:

$$(\delta\sigma_A/\delta \ln(t + c))_{T,S} = -kT/b\Delta A^* \qquad (5)$$

where t is the relaxation time and c is an integration constant approximately equal to unity. The basic assumption of these methods is that all the derivatives are evaluated at constant internal structure (which includes the mobile dislocation density and all internal stress fields) and hence that the internal stress, σ_{LR}, is a constant. If this is true, the change in the effective stress, $\delta\sigma^*$, is measured by the change in the applied stress, $\delta\sigma_A$. In the present study these relations are used to determine the activation parameters, ΔA^*, and ΔH^*, in Ni, Ni-H, Ni-C, and Ni-C-H alloys. These results are interpreted in terms of the effects of hydrogen on the thermally activated motion of dislocations.

II EXPERIMENTAL PROCEDURES

II.a Materials

The materials used are shown in Table I. Flat tensile specimens, 3 mm wide, 0.40 mm thick, and with a gauge length of 20 mm were machined from pure Ni (99.99 % purity) sheet and then were annealed in a vacuum of 5 x 10^{-5} Pa at 1473°K, followed by an anneal in 101 KPa of wet and then dry hydrogen at 1173°K for 96

hours. The Ni-H specimens were hydrogenated from the pure Ni in a fast quenching induction furnace at 1273°K and 101 KPa of H_2 for 5 to 10 minutes, quenched into a low vapor pressure oil at room temperature, and subsequently stored in liquid nitrogen. The Ni-C specimens were prepared by annealing the pure Ni in a resistance furnace at 1073°K in an atmosphere of 101 KPa of a 70/30 CO/CO_2 mixture followed by cooling to room temperature at a rate somewhat faster than a normal furnace cool. The cooling rate was fast enough to prevent the precipitation of carbide or graphite phases as monitored by TEM observations. The Ni-C-H specimens received the carbon doping and then the hydrogenation treatment. The carbon, oxygen, and nitrogen solute contents, measured by chemical

TABLE 1

INTERSTITIAL CONTENT OF DEFORMATION SPECIMENS

Material	C (appm)	O (appm)	N(appm)	H (appm) (initial)	H(appm) (after deformation)
Ni	120-140	50-60	5-10		
Ni-H	120-140	50-60	5-10	550-600	350-400
Ni-C	850-900	80-90	5-10		
Ni-C-H	650-700	80-90	5-10	600-650	400-450

analysis, are presented in Table I. Also shown in Table I is the

hydrogen concentration which was measured by a high temperature gas extraction chromatographic method both before and after the deformation experiments. Some loss of hydrogen due to outgassing during the deformation was detected. Carbon analysis indicates that some decarburization occurred during the hydrogen treatment.

II.b Deformation Experiments

Deformation experiments applied uniaxial tension utilizing an Instron machine which was vibration isolated using compressed air bags. During testing, the machine was maintained at a controlled room temperature, which varied about 0.1°K per hour. For experiments other than those at room temperature, the specimen temperature was controlled by insulating it from the grips using a thin layer of varnish and by surrounding the specimen and tensile stage with 5 cm thick Styro-Foam. The specimen temperature was established using a small resistance furnace which allowed the specimen temperature to be rapidly increased by 10 to 20°K and to be controlled to +/- 0.1°K.

Tensile experiments were performed utilizing Stress Relaxation (SR) and Differential Temperature (DT) procedures (26,30,31). Activation areas were measured using the SR method and Equation 5. The DT experiments and Equation 4 were used to measure the activation enthalpy, or "creep" enthalpy, ΔH^*. To obtain the enthalpy at zero effective stress, the "zero point" enthalpy, ΔH^*_0, the data may be integrated according to Equation 1, if σ^* is known. Alternatively the "zero point" enthalpy may be estimated by extrapolation of the enthalpy vs flow stress curve to zero

effective stress.

In order to facilitate the measurement of the activation parameters at constant structure, a sequence of deformation experiments were performed. A typical procedure would be to load a specimen to some plastic load, P_1, perform a SR test, followed by a DT test; each test being performed at the same load, P_1, plus some small increment, ΔP. After each sequence the specimen is brought to room temperature and loaded to some new plastic load, P_2 > P_1. In this fashion several sequences were performed per specimen starting at a stress near the yield point and extending to a stress near fracture.

III EXPERIMENTAL RESULTS

The effect of hydrogen and carbon on the stress relaxation in pure nickel and Ni-H alloys at low stresses is presented in Figure 1, in which typical logarithmic relaxation behavior is shown. These relaxation curves were obtained over a wide range of stresses at 300°K for all of the alloys. The linearity of the data is consistent with the assumption that the internal structure and mobile dislocation density remain constant during the relaxation. Deviations from linearity were observed after long relaxation times and were studied up to relaxation times extending to 10^6 seconds. These long time relaxations are discussed in a separate publication (31). As can be seen from the slopes of the curves in Figure 1, for times less than about 10^3 seconds, 600 appm hydrogen increases the rate of the relaxation by about a factor of about 2 compared to pure Ni. In contrast, 850 appm carbon significantly decreases the

relaxation rate. The effect of hydrogen on the relaxations in Ni-C alloys is to increase the rate of the relaxation almost to the rate characteristic of the pure Ni. At higher stresses hydrogen increases the stress relaxation in pure nickel and in Ni-C alloys to a smaller extent but the effects are still significant. The decrease of the stress relaxation rates due to carbon in pure nickel is also smaller at high stresses.

Figure 2 shows the activation area, ΔA^*, normalized to the square of the magnitude of the Burgers vector, as a function of stress for 14 different nickel and nickel hydrogen alloy specimens. The scatter associated with these results, particularly at low stresses, exceeds errors associated with the stress measurement and appears to result from variations in the internal structure, which affects the value of ΔA^*, from specimen to specimen. The effect of hydrogen is to decrease the activation area particularly at stresses between 25 to 150 MPa. At stresses above about 150 MPa the magnitude of the hydrogen effect decreases and eventually becomes negligible. Figure 2 also shows the data of Mulford (28), who measured activation areas in nickel using the strain rate change method. His results, extrapolated to low stresses, are in satisfactory agreement with the current measurements for pure nickel.

At low stresses the calculated activation areas are very large, on the order of $3000b^2$. These large magnitudes are similar to values reported in the literature (20,24,28,32) and are difficult to physically interpret. They may be associated with low

frequency thermal activation events. At the lowest stresses, the activation areas of the Ni-H alloys fall within the error bars of the values for the Ni specimens and it appears that there is no significant effect due to hydrogen. This observation agrees with the results of Eastman et al (7) who reported no hydrogen effect on the activation area in nickel in the microstrain region.

A similar analysis of the effect of carbon in pure nickel is presented in Figure 3. As shown, the effect of carbon is to increase the activation areas in nickel; particularly at low stresses. This effect of carbon solutes agrees with the observed decreases in the strain rate sensitivity due to carbon solutes which were discussed by Kocks et al (22). The effect of hydrogen on the activation areas in Ni-C alloys is to reduce the activation areas to values similar to those of pure Ni (Figure 4). Hydrogen solutes appear to reduce the effect caused by carbon solutes. These results are summarized in Figure 5, in which smooth curves were drawn through the data for Ni, Ni-H, Ni-C, and Ni-C-H.

The plastic strain rates, $\dot{\epsilon}_p$, during stress relaxation are higher in the Ni-H alloys and lower in the Ni-C alloys compared with the pure nickel specimens tested under identical conditions, that is,

$$\dot{\epsilon}_p^{Ni-H} > \dot{\epsilon}_p^{Ni} \approx \dot{\epsilon}_p^{Ni-C-H} > \dot{\epsilon}_p^{Ni-C}$$

while the activation areas for identical testing conditions are:

$$\Delta A^{*Ni-H} < \Delta A^{*Ni} \approx \Delta A^{*Ni-C-H} < \Delta A^{*Ni-C}.$$

The increase in the thermally activated plastic strain rate and the decrease in the activation area, ΔA^*, caused by hydrogen and the

corresponding decrease in plastic strain rate and increase in ΔA^* caused by carbon appear to be inconsistent with Equation 1 if all other activation parameters remained unaffected by the solute additions. Equation 1 taken with the experimental observations requires that ΔH^* decreases due to hydrogen and increases due to carbon. Hence the implied effect of hydrogen is to decrease ΔH^*_0 and of carbon to increase ΔH^*_0.

The effects of hydrogen and carbon on the activation enthalpies ΔH^* and ΔH^*_0 were determined using thermal cycling experiments (Equation 4) in combination with the activation area measurements using the relation:

$$\Delta H^* = -(\Delta\sigma_A/\Delta T)_\epsilon bT\Delta A^*. \tag{6}$$

In these experiments the temperature dependence of the effective stress at 300°K was measured as a function of stress (Figures 6 and 7). For the alloys studied, the term $(\Delta\sigma_A/\Delta T)_\epsilon$ is approximately constant, independent of strain hardening, which is consistent with the Cottrell-Stokes Law (33). The data fall within a scatter band about a mean value of 0.035 MPa/°K for Ni, Ni-H, and Ni-C-H, and about 0.030 MPa/°K for Ni-C. These data show that 600 appm hydrogen has little effect on the temperature dependence of the flow stress in "pure" nickel, while carbon decreases $(\Delta\sigma_A/\Delta T)_\epsilon$ about 15 percent. Adding H to the Ni-C alloy increases $(\Delta\sigma_A/\Delta T)_\epsilon$ by about 15 percent to the value characteristic of "pure" Ni.

The data on the temperature dependence of the flow stress were combined with the activation area results to derive measurements of the activation enthalpy, ΔH^*, as a function of stress (Figure 8).

The activation enthalpy, ΔH^*, monotonically decreases with increasing stress as expected from Equation 1. The effect of hydrogen is to reduce the activation enthalpy for dislocation motion in Ni and Ni-C with the effect being is largest at low stresses. Carbon increases the activation enthalpy for dislocation motion in nickel with the largest effect found at the lowest stresses.

An estimate of the total enthalpy, ΔH^*_0, was obtained by extrapolating the enthalpy-stress data in Figure 8 to zero applied stress. This extrapolation, which should be to zero effective stress, overestimates the total enthalpy. The results indicate a total activation energy, ΔH^*_0, of 1.9 eV for Ni, 1.4 Ev for Ni-H, 2.9 eV for Ni-C, and 2.0 eV for Ni-C-H alloys with an error of +/- 0.4 eV. These estimates can be compared with total activation enthalpies for dislocation motion in other FCC metals and alloys. Values between 1.7 and 3.4 eV have been measured for Al-3%Mg alloys at 300°K (34) and 1.25 and 1.15 eV have been reported for pure aluminum (26) and copper (35), respectively. The present values are consistent with those measured in other FCC systems.

IV DISCUSSION

The experimental results clearly show that hydrogen in solid solution increases the rate of stress relaxation in pure Ni and in Ni-C alloys. This experimental observation is consistent with stress relaxation measurements carried out on steels and iron during cathodic charging (36-39). The cathodic charging experiments are however troubled by lattice damage during the cathodic

polarization which can introduce dislocations and dislocation sources into the surface regions of the specimen. This is not a difficulty with the present experiments as TEM examination of the specimens did not inuicate any increased dislocation density due to specimen preparation. Despite the effect of hydrogen in increasing the stress relaxation rate, Lunarska (36) interpreted the result as being due to a decrease in the dislocation velocity stress expo.ient and Oriani (37-39) related the effect to the growth of microvoids. Neither of the two previous studies determined the parameters which characterize the dislocation response to stress and temperature.

The present experimental results clearly show that the effects of hydrogen on stress relaxation are due to changes in the activation area, ΔA^*, and the activation enthalpy, ΔH^*_0, associated with hydrogen in solid solution. These effects are summarized in Table II. The increased relaxation rate is caused by an increased dislocation mobility for a given stress and temperature. In both pure Ni and Ni-C alloys, hydrogen decreases the activation area, ΔA^*, over a wide range of stress and decreases the activation enthalpy, ΔH^*_0. The net effect of hydrogen is to decrease the activation enthalpy,

$$\Delta H^* = (\Delta H^*_0 - \int b\Delta A^* \delta\sigma^*) \qquad (7)$$

and therefore to increase the dislocation velocity, v_d, given by:

$$v_d = (\dot{\epsilon}_0/\rho_m b)\exp{-(\Delta H^*/kT)} \qquad (8)$$

The increased stress relaxation rate, which implies a decrease in ΔH^*, indicates that the magnitude of the decrease in ΔH^*_0 is greater than that of the stress dependent term involving ΔA^*, in agreement

with the derived values of these parameters.

TABLE II

Summary of Hydrogen and Carbon effects on the Activation Parameters for Dislocation Motion in Nickel.

	Ni	Ni-H	Ni- C	Ni-C-H
$\dot{\epsilon}_p \ / \ \dot{\epsilon}_p^{Ni}$	1	> 1	< 1	- 1
$\Delta A^* \ / \ \Delta A^{*Ni}$	1	< 1	> 1	- 1
$\Delta H^* \ / \ \Delta H^{*Ni}$	1	< 1	> 1	- 1
$\Delta H^*_0 (eV)$	1.9	1.4	2.9	2.0

Increases in dislocation velocity due to hydrogen have been directly observed in a wide variety of systems using environmental cell TEM methods (2-4,40). In the Ni (2,5) and Fe (3) systems the hydrogen enhancement of dislocation velocities are greater in specimens which contain interstitials in solid solution, i.e. in which the solute interstitials provide the major dislocation barriers. Direct observations of dislocation mobility suggest that solute hydrogen, introduced by a gaseous H_2 atmosphere at a pressure of 13 Kpa, can cause an increase of velocity by a factor of about 10 at 300°K. Using Equation 8, this corresponds to a hydrogen caused decrease of ΔH^*, $\delta(\Delta H^*)$ = -0.06 eV. This is comparable to the decrease in ΔH^* caused by H in the intermediate stress range studied (Figure 8). Since the direct TEM observations were carried out at H_2 pressures which correspond to a solute hydrogen concentration of about 3 appm, the H effect on ΔH^* may be

expected to be greater in the present alloys, which contain about 600 appm hydrogen. Estimates of the effect of hydrogen on dislocation velocities in the present experiments can be obtained using the changes in ΔH^* at an applied stress, σ_A, (Figure 8) correspond to the calculated (Equation 8) ratios of the dislocation velocities in the absence of H, v_d, to those in the alloys containing H, v^H_d. These results are given in Table III, where it is evident that the hydrogen effect is strongly dependent on the applied stress.

TABLE III

Effect of Hydrogen on the Activation Enthalpy and the Dislocation Velocity

	σ_A (Mpa)	$\delta \Delta H^*$ (eV)	v^H_d / v_d
Pure Ni	50	− 0.32	3×10^5
Pure Ni	100	− 0.11	81
Pure Ni	150	− 0.05	7
Ni-C	50	− 0.49	3×10^8
Ni-C	100	− 0.13	181
Ni-C	150	− 0.06	11

Increases in dislocation velocities due to H have been observed in BCC (1), FCC (2), HCP (4) crystal systems and in pure metals (1-3) and alloys (4,40). They have also been observed in precipitation hardened (41) as well as in solid solution alloys. In addition, the enhanced velocity has been observed for isolated dislocations, for dislocations which are intersected by forest

dislocations, and for screw, edge, and mixed character dislocations. Thus, the effect is a very general one and the mechanism which accounts for the H enhanced velocity must also be one which is generally applicable to a variety of systems. One such mechanism is the concept of "hydrogen shielding" of the elastic interactions between dislocations and other localized stress fields (42). These local stress fields, which provide barriers to dislocation motion, can be provided by solutes, intersecting dislocations, small precipitates, etc. and hence generally control dislocation motion in a wide range of systems.

Interaction of mobile dislocations with these short range elastic barriers can be described by thermally activated motion over the barriers (Equations 1-5). In the absence of H, the height and shape of the barrier is determined by the elastic interactions between the dislocation and the pinning point. These are the parameters ΔH^* and ΔA^* which are determined in the pure Ni and the corresponding parameters determined in the Ni-C alloy. In the pure Ni, the dominant barriers are probably forest dislocations, while in the Ni-C alloy the barriers are probably forest dislocations, C interstitials, and small C clusters. Addition of H to the Ni and the Ni-C alloy allows H atmospheres to develop at the mobile dislocations, at the forest dislocations, and in the stress fields of C solutes and small C clusters.

While the binding enthalpy of H to dislocations has not been determined for FCC metals, it is expected to be of the order of 0.1 eV (12). For a binding enthalpy, B, of 0.1 eV and the lattice H

concentration, C_L, of 600 appm, the enhancement factor, C_D/C_L, of the H concentration in the vicinity of the dislocations, C_D, can be estimated to be 48.0 at 300°K from the relation:

$$C_D/C_L = \exp(B/kT) \tag{9}$$

From Robertson's data (43), the diffusivity of H in Ni, D_H, at 300°K is calculated to be 6.6 X $10^{-14}m^2$/sec. Using the concept of a drift velocity for a dislocation atmosphere (44) we can estimate that the dislocation velocity, V_c, at which the dislocation breaks away from its H atmosphere is:

$$V_c = 4D_H kT/Br_c, \tag{10}$$

where r_c is the dislocation core radius, is about 2.3 X $10^{-4}m$/sec. The critical strain rate, ϵ_c, corresponding to this critical break-away velocity can be estimated from:

$$\dot{\epsilon}_c = \rho_m bV_c \tag{11}$$

where b is the magnitude of the Burgers vector. For a mobile dislocation density, ρ_m, of $10^{10}/m^2$ the strain rate below which the H atmospheres can move with the dislocations is $\dot{\epsilon}_c = 6.8$ X$10^4 sec^{-1}$.

The response of the dislocations to the presence of the H atmospheres (25) is dependent on the temperature and strain rate. At "low" temperatures and at a strain rate where the H atmospheres move with but lag behind the dislocations, they exert a drag force on the dislocations and result in increases in the yield stress. At somewhat higher strain rates (or lower temperatures), the dislocations can break away from the atmospheres and serrated yielding is observed. As the temperature is increased, the strain rates at which the atmospheres can move with the dislocations

increases, but the enhancement factor of H at the dislocation is decreased. At a given strain rate, the drag force on the dislocation due to the H atmosphere decreases as the temperature increases due to the decreased H concentration enhancement and the increased drift velocity. Consequently, under conditions where the H atmospheres can move with the dislocations, little direct drag effect on the dislocations is noted. This appears to be the case for Ni at 300°K and at low strain rates, $\dot{\epsilon} \leq 1 \times 10^{-4}$ sec^{-1}.

In addition to the above very general responses of the dislocation to the presence of H atmospheres, "hydrogen shielding" will occur under the temperature and strain rate conditions which allow the motion of H atmospheres with the dislocations. These shielding effects act to minimize the elastic interactions of the dislocations with the localized stress fields of the obstacles. Under these conditions, the total interactions which must be accounted for are:

a. Between the moving dislocation and the elastic stress barrier.

b. Between the H solutes in the atmosphere and the elastic stress barrier.

c. Between the H solutes in the atmosphere around the elastic barrier and the moving dislocation.

d. Between the H solutes in both atmospheres.

The latter three of these interactions will be most important when the moving dislocation interacts with forest dislocations as both can then accumulate significant H atmospheres. In addition to these

terms, the distribution of H in the atmospheres will change as the dislocation approaches the elastic stress barrier since the H concentration at any point reflects the total stress at that point (both from the dislocation and from the barrier stress field). Detailed calculations have shown that significant rearrangement of the H solutes occurs as the dislocation approaches the barrier (42). The net effect is that the mobile H solutes rearrange themselves to minimize the total energy of the system and this has the effect of "shielding" the dislocation from the elastic stress field of the barrier thereby reducing the interaction forces between the dislocations and the barriers.

The present results are consistent with this model of "hydrogen shielding". In the presence of H, the zero effective stress activation enthalpy, ΔH^*_0, is decreased for pure Ni, where the barriers are probably forest dislocations, and for Ni-C, where the barriers are presumably C interstitials. "Hydrogen shielding" is expected to decrease the interaction energy for both of these barriers (42). Furthermore, since the H atmosphere interactions vary approximately as r^{-2}, and the elastic interactions of the barriers with the dislocations vary as r^{-1}, the effect of "hydrogen shielding" is to decrease the range of the interaction which is equivalent to decreasing the activation area, ΔA^*, as experimentally observed.

IV CONCLUSIONS

1) Stress relaxation studies of Ni, Ni-H, Ni-C, and Ni-C-H alloys have shown that hydrogen in solid solution increases the rate of

stress relaxation, while carbon decreases the relaxation rate. These effects are most pronounced at low stresses and decrease with increasing prestrain.

2) Thermal activation analysis of the stress relaxation results have shown that hydrogen reduces the "activation area", while carbon increases the "activation area" which characterizes the dislocation mobility.

3) Hydrogen also decreases the zero effective stress activation enthalpy, ΔH^*_0, for dislocation motion, while carbon increases this parameter.

4) The zero effective stress enthalpies, ΔH^*_0, are 1.9 eV for Ni, 1.4 eV for Ni-H, 2.9 eV for Ni-C, and 2.0 eV for Ni-C-H alloys with an error of +/- 0.4 eV.

5) The activation enthalpy which characterizes the stress relaxation is decreased at all stresses by the addition of H to Ni and Ni-C alloys.

6) The reduction in the activation enthalpy for dislocation motion by hydrogen in Ni and Ni-C alloys is attributed to dynamic attractive interactions between mobile hydrogen atmospheres associated both with the gliding dislocations and with the strain field of the pinning obstacles, i.e. to "hydrogen shielding" of the elastic interactions between mobile dislocations and the elastic stress fields of dislocation and C interstitial barriers.

ACKNOWLEDGEMENT

REFERENCES

1) T. Tabata and H. K. Birnbaum, Scripta Metall. **18**, 231 (1984).

2) I. M. Robertson and H. K. Birnbaum, Acta Metall. **34**, 353 (1986).

3) G. Bond, I. M. Robertson and H. K. Birnbaum, Acta Metall. **36**, 2193 (1988).

4) D. Shih, I. M. Robertson and H. K. Birnbaum, Scripta Metall. **36**, 111 (1988).

5) C. D. Beachem, Metall. Trans. **3**, 437 (1972).

6) T. Matsumoto, J. Eastman and H. K. Birnbaum, Scripta Metall. **15**, 1035 (1981).

7) J. Eastman, F. Heubaum, T. Matsumoto and H. K. Birnbaum, Acta Metall. **30**, 1579 (1982).

8) A. Kimura and H. K. Birnbaum, Acta Metall. **35**, 1077 (1987).

9) H. Matsui, H. Kimura and S. Moriya, Mat. Sci. Eng. **40**, 207 (1979).

10) S. Moriya, H. Matsui and H. Kimura, Mat. Sci. Eng. **40**, 217 (1979).

11) H. Matsui, H. Kimura and Akihiko Kimura, Mat. Sci. Eng. **40**, 227 (1979).

12) T. Broniszewski and G. S. Smith, Acta Metall. **11**, 165 (1963).

13) A. H. Windle and G. S. Smith, Metal Sci. J. **4**, 136 (1970).

14) D. Ulmer, Ph.D. Thesis, University of Illinois at Urbana - Champaign, (1988).

15) L. Zwell E. J. Fasiska, Y. Nakada and G. S. Keh, Trans. TMS-AIME **242**, 765 (1968).

16) G. J Thomas and W. D. Drotning, Metall. Trans. **14A**, 1545

(1983).

17) H. J. Bauer, G. Berninger and G. Zimmerman, Z. Naturforsch; **23a,** 2023 (1968).

18) H. Peisl, in <u>Hydrogen in Metals</u> Vol. I, Ed. by G. Alefeld and J. Volkl, Springer-Verlag, Berlin, p. 53, (1978).

19) S. Diamond and C. Wert, Trans. TMS-AIME **239,** 705 (1967).

20) D. E. Sonon and G. V. Smith, Trans. TMS-AIME **242,** 1527 (1968).

21) Y. Nakada and A. S. Keh, Metall. Trans. **2,** 441 (1971).

22) U. F. Kocks, R. E. Cook and R. A. Mulford, Acta Metall. **33,** 623 (1985).

23) Y. Nishino, T. Kato, S. Tamaoka and S. Asano, Scripta Metall. **21,** 1235 (1987).

24) K. Tanaka, T. Inukai, K. Uchida and M. Yamada, J. Appl. Phy. **54,** 6890 (1983).

25) A. Kimura and H.K. Birnbaum, Acta Metall. **38,** 1343 (1990).

26) A. G. Evans and R. D. Rawlings, Phy. Stat. Sol. **34,** 9 (1969).

27) U. F. Kocks, A. S. Argon, and M. F. Ashby, in <u>Progress in Materials Science</u>, Vol. 19, Pergamon Press, Oxford, (1975).

28) R. A. Mulford, Acta Metall. **27,** 1115 (1978).

29) R. W. Balluffi and A. V. Granato, in <u>Dislocations in Solids</u>, Vol. 4, Ed. by F. R. N. Nabarro, North-Holland, (1979).

30) V. I. Dotensko, Phy. Stat. Sol. **93,** 11 (1979).

31) E. Sirois, PhD Thesis, University of Illinois at Urbana-Champaign, (1990).

32) M. E. Kassner and A. K. Mukherjee, Scripta Metall. **17,** 741 (1983).

33) S. J. Basinski and Z. S. Basinski, in <u>Dislocations in Solids</u>, Vol. 4, Ed. by F. R. N. Nabarro, North-Holland, (1979).

34) Walton, L. A. Shepard and J. E. Dorn, Trans. ASM **52**, 494 (1960).

35) J. Bonneville, B. Escaig and J. L. Martin, Acta Metall. **36**, 1989 (1988).

36) E. Lunarska, Scripta Metall. **11**, 283 (1977).

37) R. A. Oriani and P. H. Josephic, Acta Metall. **27**, 997 (1979).

38) R. A. Oriani and P. H. Josephic, Scripta Metall. **13**, 469 (1979).

39) R. A. Oriani, Corrosion, NACE **43**, 390 (1987).

40) P. Rozenak, I. M. Robertson and H. K. Birnbaum, Acta Metall. **38**, 2031 (1990).

41) G. Bond, I. M. Robertson and H. K. Birnbaum, Acta Metall. **35**, 2289 (1988).

42) H. K. Birnbaum, P. Sofronis and R. McMeeking, To Be Published.

43) W. Robertson, Z. fur Metallkunde, **64**, 436 (1973).

44) A. H. Cottrell, Phil. Mag. **44**, 829 (1953).

FIGURE CAPTIONS

1. Stress relaxation results showing $-\Delta\sigma$ vs Log(t), for Ni (0), Ni-600 appm H (●), Ni-850 appm C (Δ), and Ni-700 appm C-600 appm H (▲) alloys at 30 MPA and 300°K.

2. Stress relaxation results showing the activation area normalized by the square of the Burgers vector vs applied stress for Ni (0) and Ni-600 appm H (●) alloys at 300°K and for Ni (Ref. 24) (——)

3. Stress relaxation results showing the activation area normalized by the square of the Burgers vector vs applied stress for Ni (0) and Ni-850 appm C (Δ) alloys at 300°K.

4. Stress relaxation results showing the activation area normalized by the square of the Burgers vector vs applied stress for Ni-850 appm C (Δ) and Ni-700 appm C-600 appm H (▲) alloys at 300°K.

5. Summary of the stress relaxation results showing the activation area normalized by the square of the Burgers vector vs applied stress for Ni (——), Ni-600 appm H (•••), Ni-850 appm C (— • — •), and Ni-700 appm C-600 appm H (— •• — ••), alloys at 300°K. The error bars are indicated by vertical lines.

6. Differential temperature test results showing $(\Delta\sigma^*/\Delta T)_\varepsilon$ vs applied stress for Ni (0) and Ni-600 appm H (●) alloys, at 300°K.

7. Differential temperature test results showing $(\Delta\sigma^*/\Delta T)_\epsilon$ vs applied stress for Ni (O), Ni-850 appm C (Δ) and Ni-700 appm C-600 appm H (▲) alloys at 300°K.

8. Thermal activation analysis results showing the activation enthalpy vs applied stress for Ni (——), Ni-600 appm H (····), Ni-850 appm C (— · — ·), and Ni-700 appm C-600 appm H (— ·· — ··) alloys measured at 300°K. The error bars are indicated by vertical lines.
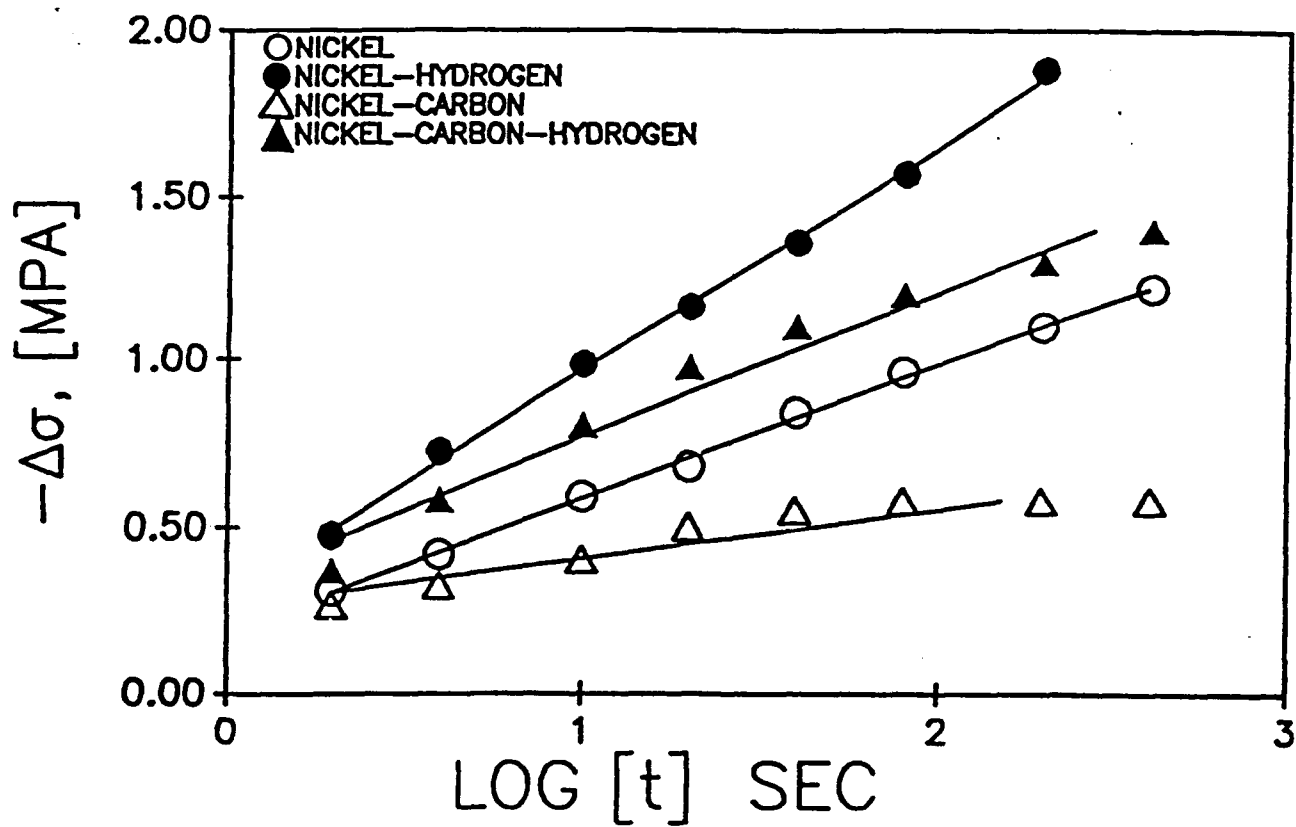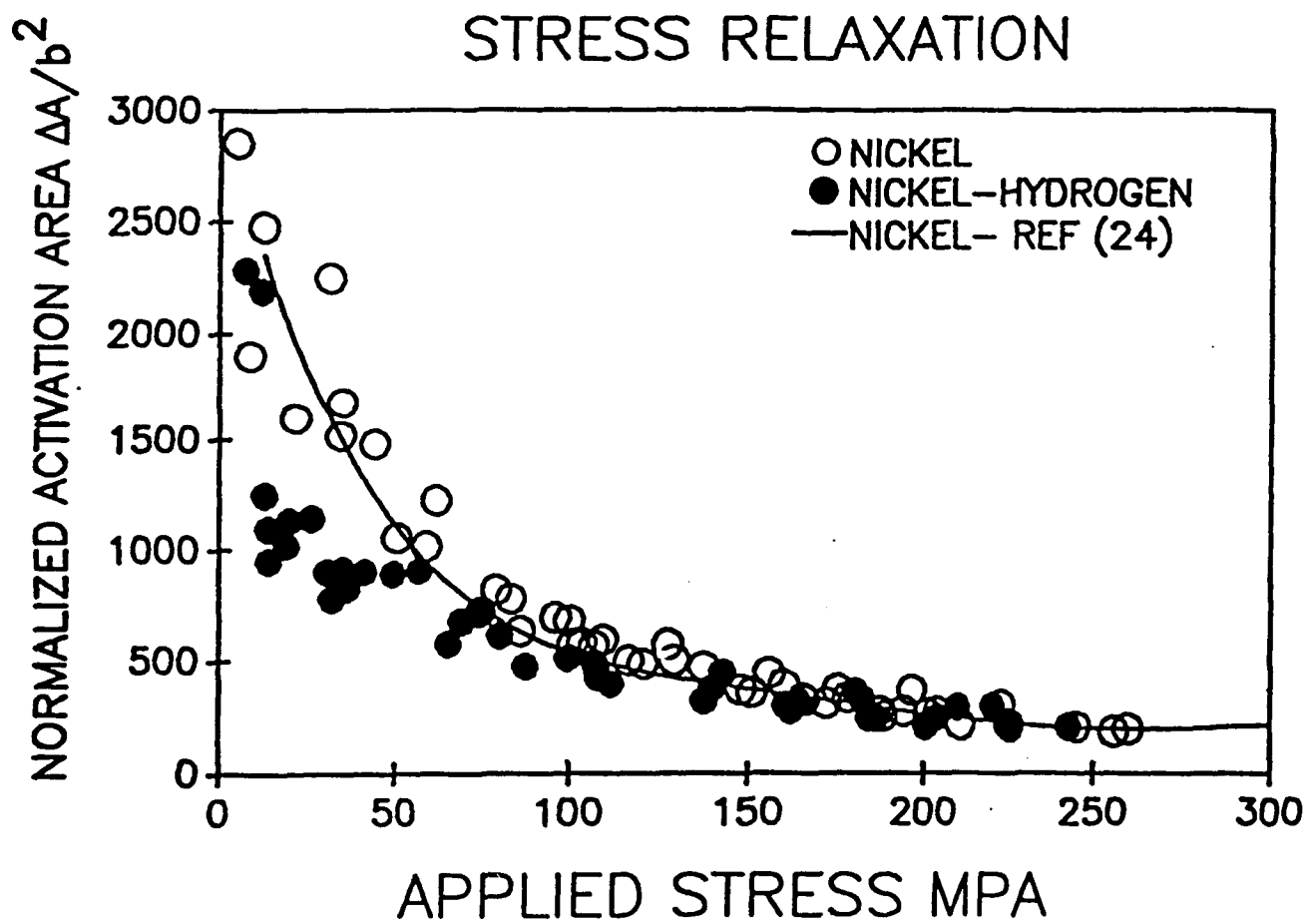
STRESS RELAXATION

Legend:
○ NICKEL
● NICKEL–HYDROGEN
△ NICKEL–CARBON
▲ NICKEL–CARBON–HYDROGEN

Y-axis: $-\Delta\sigma$, [MPA]

X-axis: LOG [t] SEC

Fig. 1

STRESS RELAXATION

Fig. 2

STRESS RELAXATION

Fig. 3

STRESS RELAXATION

Fig. 4

THERMAL ACTIVATION ANALYSIS
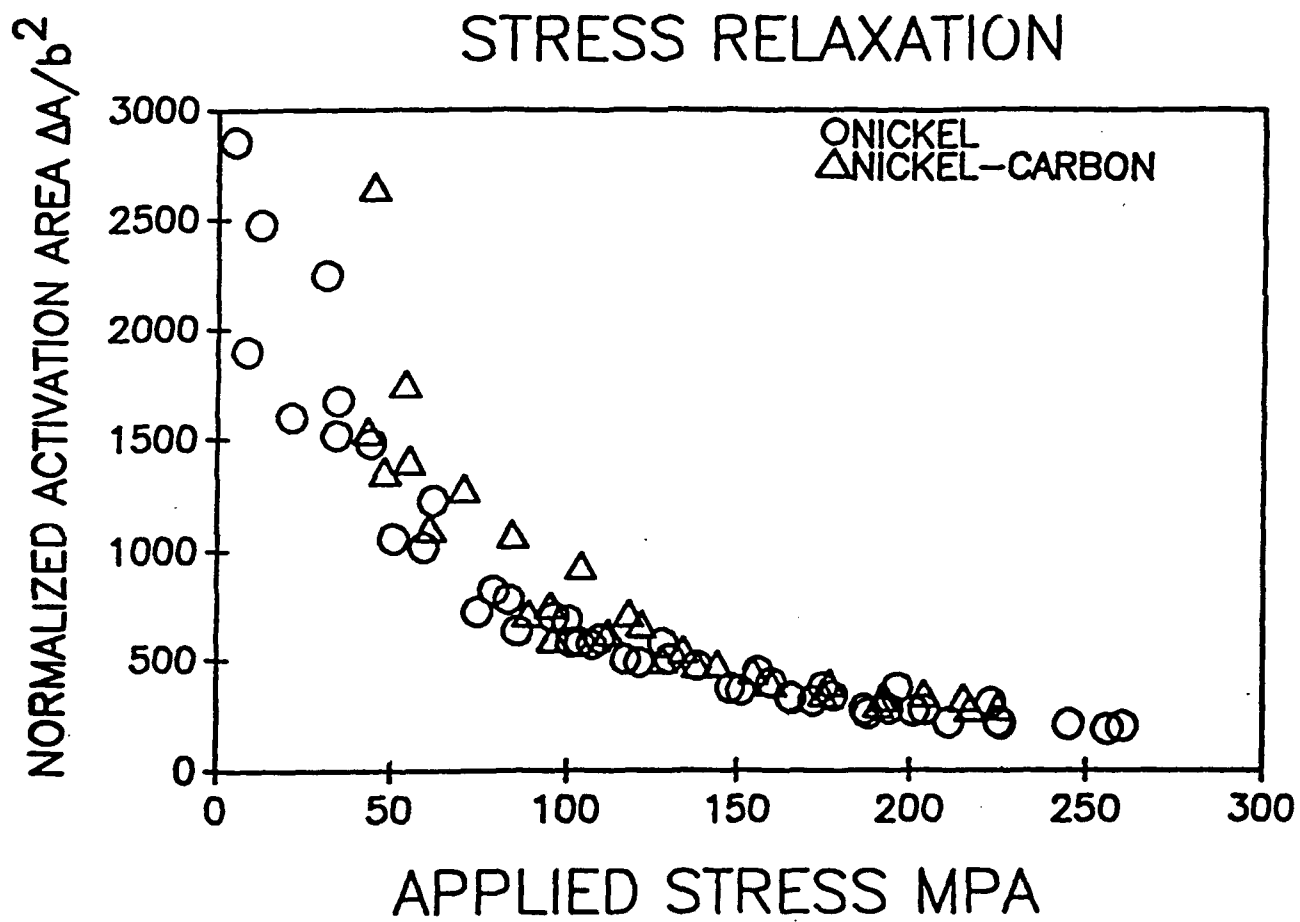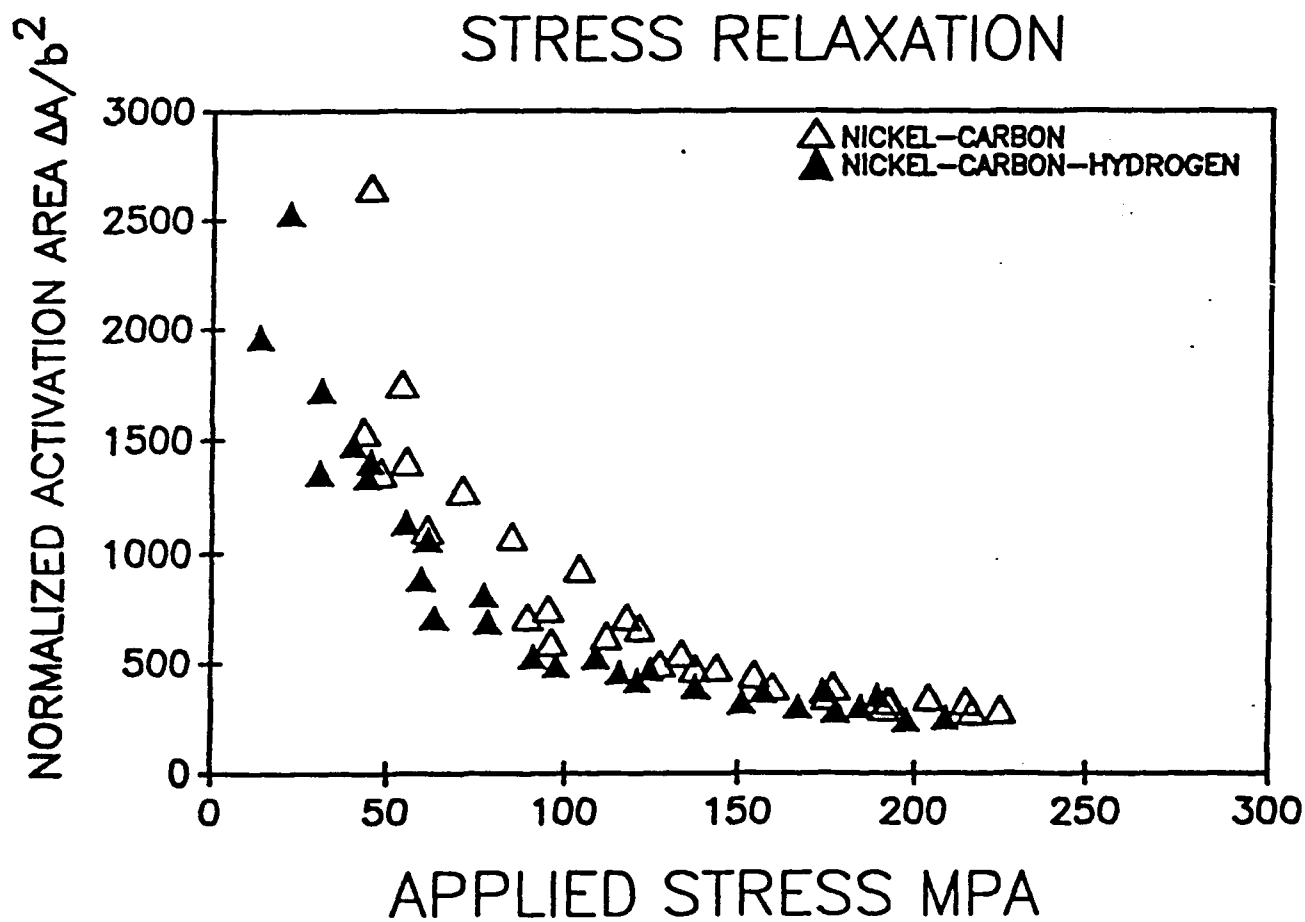
Fig. 5

THERMAL ACTIVATION ANALYSIS
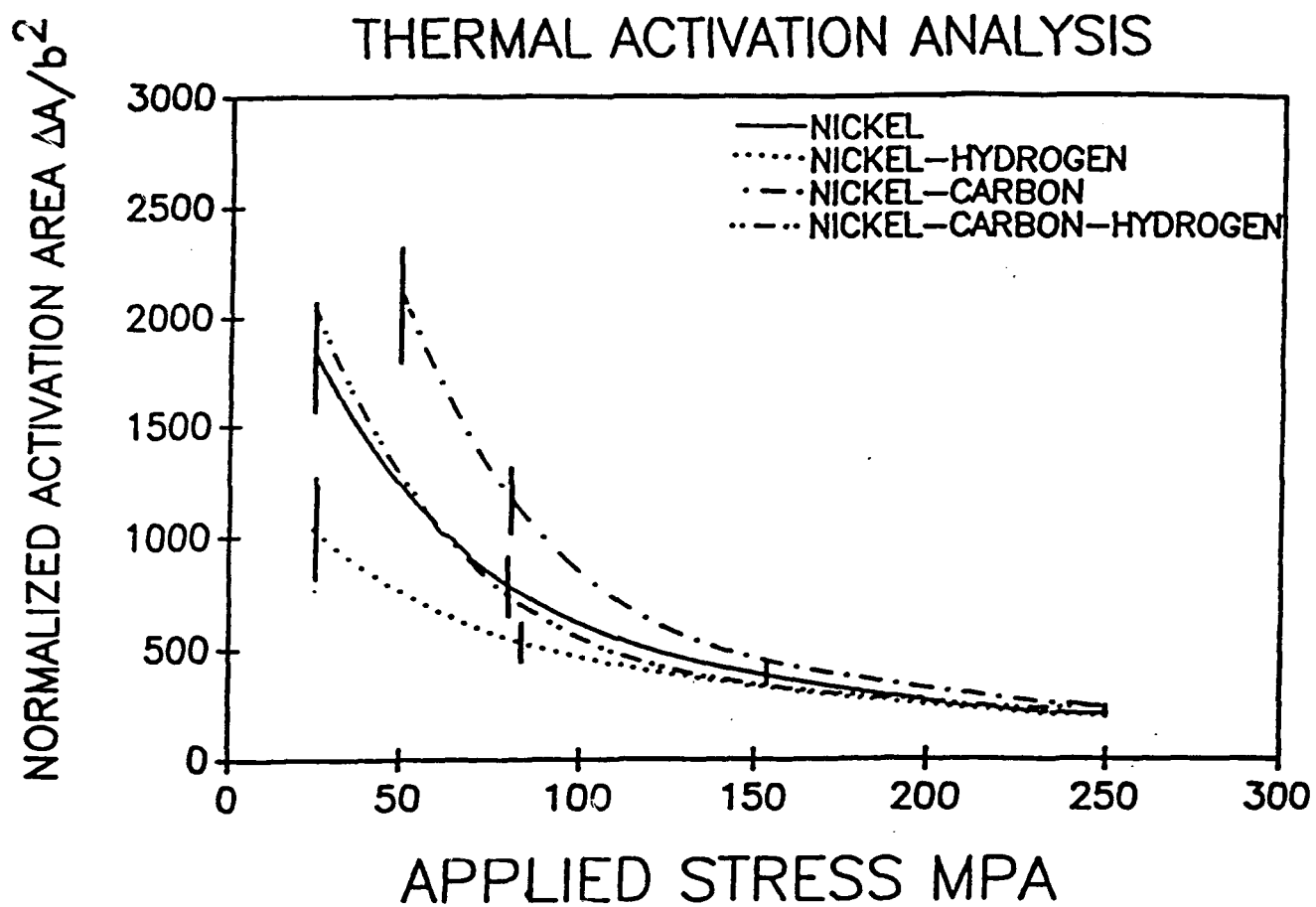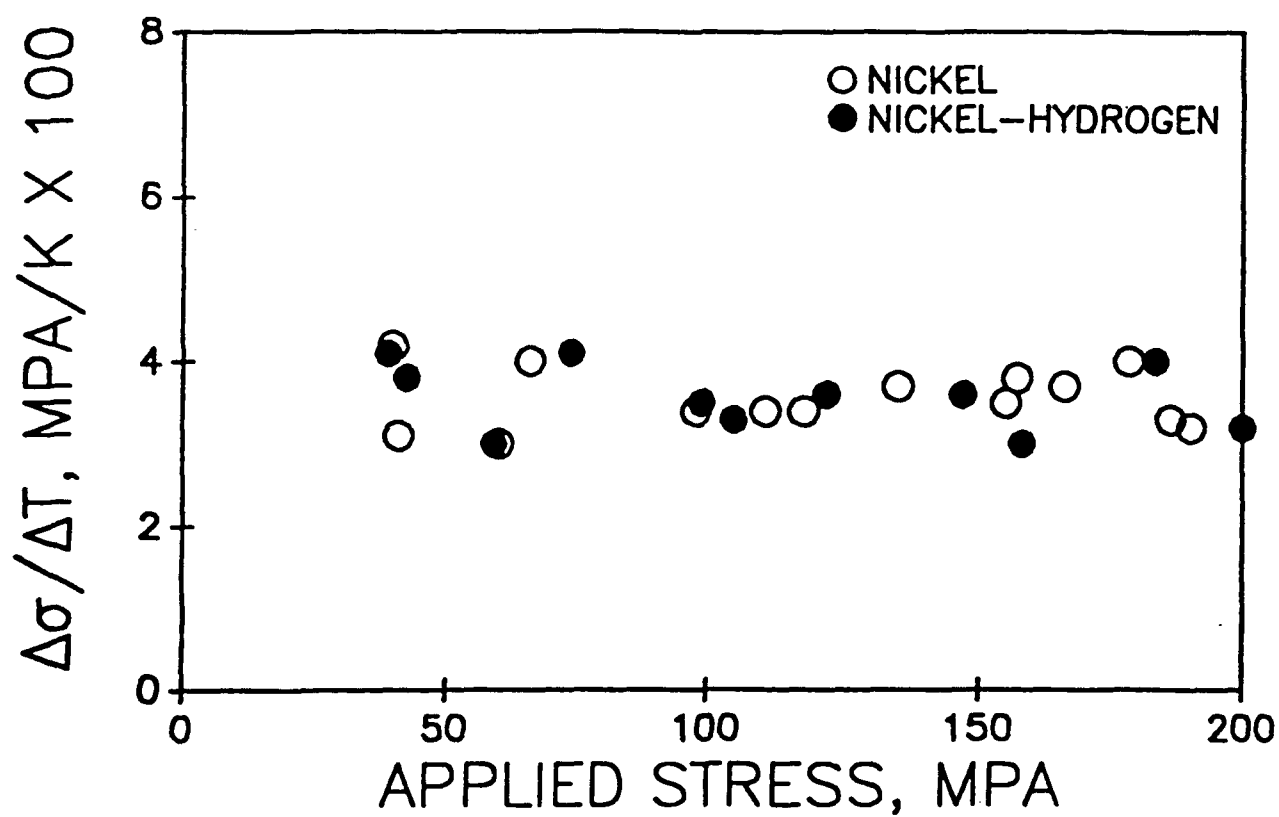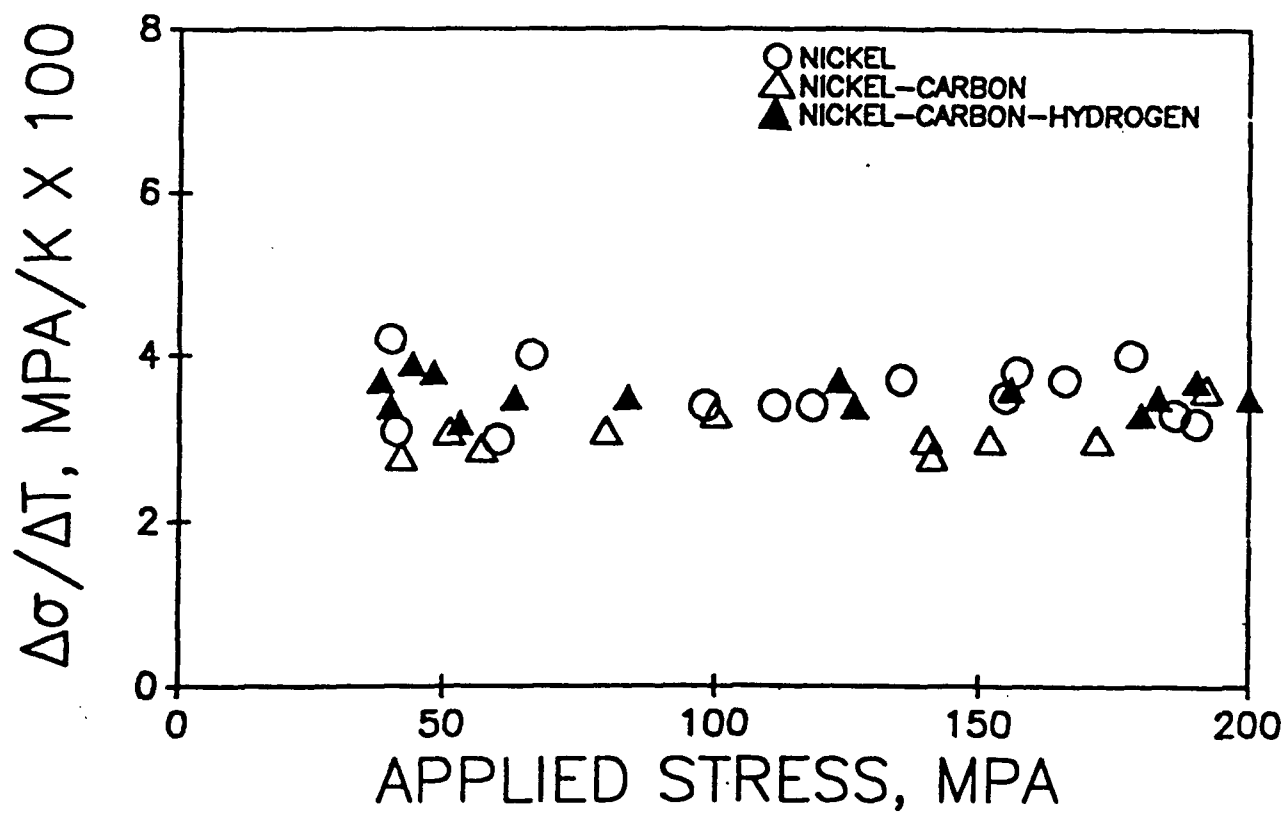

Fig. 6

THERMAL ACTIVATION ANALYSIS

Fig. 7
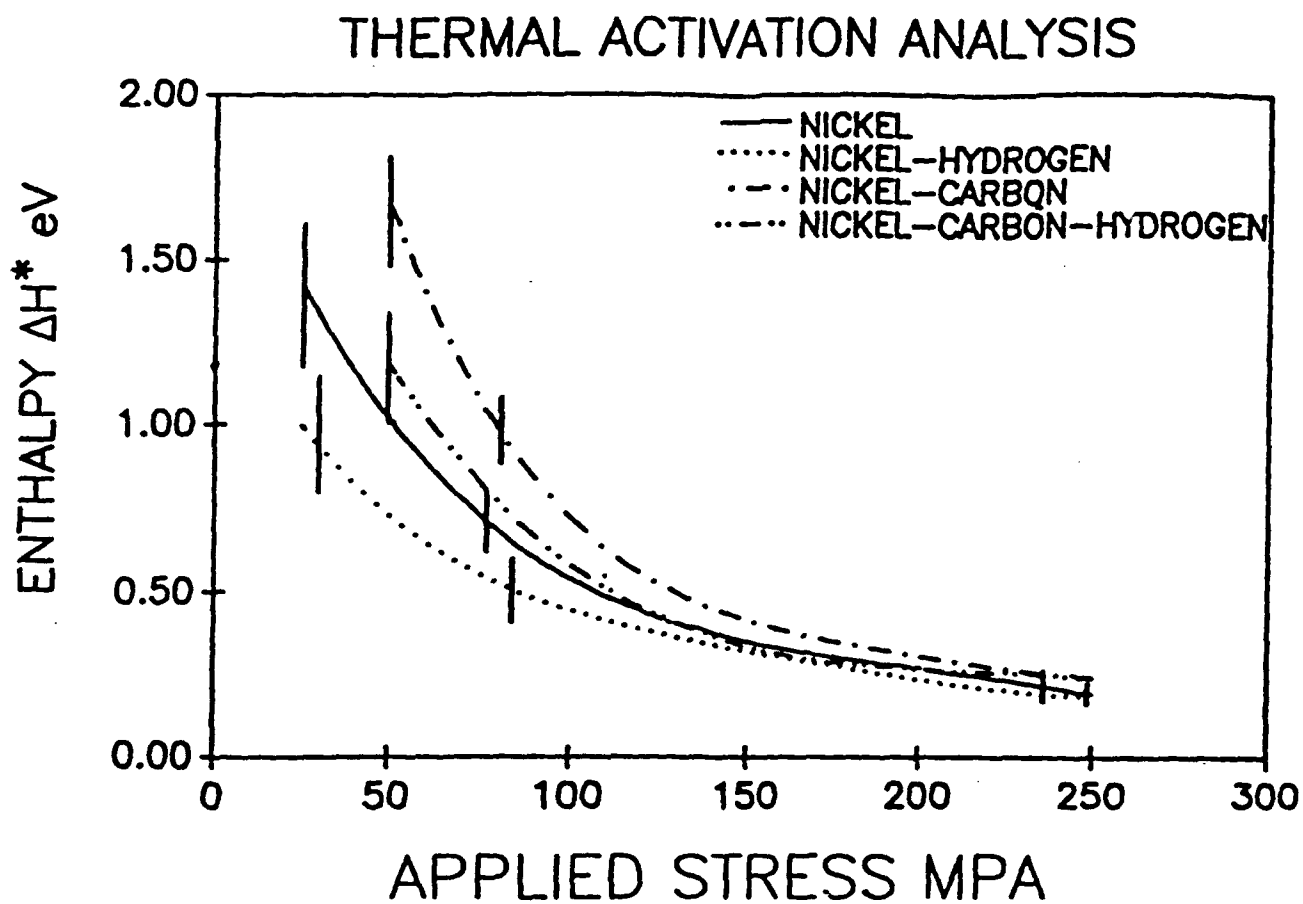
THERMAL ACTIVATION ANALYSIS

Fig. 8